

## A Posteriori Error Estimation and Adaptive Node Refinement for Fast Moving Least Square Reproducing Kernel (FMLSRK) Method

Chany Lee<sup>1</sup>, Chang-Hwan Im<sup>2</sup>, Hyun-Kyo Jung<sup>3</sup>, Hong-Kyu Kim<sup>4</sup> and Do Wan Kim<sup>5</sup>

**Abstract:** In the present study, a residual-based a posteriori error estimation for a kind of meshless method, called fast moving least square reproducing kernel (FMLSRK) method is proposed. The proposed error estimation technique does not require any integration cells in evaluating error norm but recovers the exact solutions in a virtual area defined by a dilation parameter of FMLSRK and node density. The proposed technique was tested on typical electrostatic problems with gird or random node sets and the simulation results show that the proposed error estimation technique can be applied to adaptive node refinement process for more efficient meshless analysis of electromagnetic field.

**Keyword:** Adaptive node refinement, electrostatics, error estimation, fast moving least square reproducing kernel (FMLSRK) method, meshless methods.

### 1 Introduction

Finite element method (FEM) has been widely used in various scientific and engineering fields to solve partial differential equations. FEM, however, has some defects such as time consuming mesh generation and difficulty in treating small or sophisticated objects inside a large analysis domain. To tackle such problems, recently, various kinds of meshless methods have been developed and introduced. For instances, smoothed particle hydrodynamics (SPH) and element free Galerkin

method (EFG) were developed by Gingold et al. [Gingold, R. A.; Monaghan, J. J. (1997)] and Belytschko et al. [Lu, Y. Y.; Belytschko, T.; Gu, L. (1994)], respectively. Reproducing kernel particle method (RKPM) [Liu, W. K.; Jun, S.; Zhang, Y. F. (1995)] and moving least square reproducing kernel (MLSRK) method [Liu, W. K.; Li, S.; Belytschko, T. (1996)] by Liu et al., partition of unity finite element method (PUFEM) by Melenk et al. [Melenk, J. M.; Babuška, I. (1996)], and h-p Clouds by Duarte et al. [Duarte, C. A.; Oden, J. T. (1996)] are also popular examples of the meshless methods. Particularly, the meshless local Petrov-Galerkin method(MLPG) and local boundary integral equation method(LBIE)[Atluri, S.N.; Kim, H.G.; Cho J.Y.(1999)] deserve mentioning, in which local weak form on the local sub-domain defined at each node in a computational domain is used in conjunction with the penalty approach for the essential boundary condition. The MLPG method is extended to solving the convection diffusion [Lin H.; Atluri S.N. (2000)] and viscous flow [Lin H.; Atluri S.N. (2001)] problems, including the study on efficiency for a variety of this method[Atluri S.N.; Shen S. (2002)]. More recently, Kim et al. proposed fast moving least square reproducing kernel (FMLSRK) method [Kim, D. W.; Kim, Y. (2003)], [Kim, D. W.; Kim, H. K. (2004)]. Basically, the method was based on the concepts of the MLSRK method, but it had improved characteristics such that both shape functions and all of their derivatives could be evaluated simultaneously within a single equation, which made the analysis procedure computationally more efficient. In case higher order derivative approximation is needed as in a meshfree point collocation strategy, the radial basis function could be a candidate but its process is complicated, so that

<sup>1</sup> Seoul National University, Seoul, Korea.

<sup>2</sup> Corresponding author. Dept. Biomedical Eng., Yonsei University, Wonju, Korea.

<sup>3</sup> Seoul National University, Seoul, Korea.

<sup>4</sup> Korea Electrotechnology Research Institute, Changwon, Korea.

<sup>5</sup> Hanyang University, Ansan, Korea.

RBF-based differential quadrature method is proposed to circumvent this complexity, which works as similar as the finite difference method [Shu C.; Ding H.; Yeo K.S. (2005)].

The meshless methods do not need to generate finite elements, but place finite number of nodes to get approximated solutions. Since the solution accuracy of FEM is significantly affected by quality of meshes, the meshless methods are promising for the problems with small objects inside a large analysis domain, moving objects, very sophisticated geometry, and so on, for which high-quality finite elements are hardly obtained. Furthermore, adaptive strategy can be more readily implemented in the meshless methods, because one just needs to place new nodes on higher error regions without generating new mesh structures.

The adaptive meshless analysis is relatively more important than the adaptive finite element analysis because the influence region of a shape function in most meshless methods is overlapped with its neighboring ones, which results in less sparse matrix than that of FEM and thus yields considerable computational burden. Hence, in order to reduce size of node set and enhance computational efficiency, adaptive node refinement is of great necessity.

Both FEM and meshless methods need to estimate error distributions to adaptively refine meshes or nodes. While significant number of studies have been performed to estimate a priori or a posteriori error distribution of finite element solutions, such as super-convergent patch recovery (SPR), recovery by equilibrium in patches (REP) and so on [Bugeda, G. (2002)], [Boroomand, B.; Zienkiewicz, O. C. (1997)], [Ubertini, F. (2004)], [Kvamsdal T.; Okstad, K. M. (1998)], the error estimators for meshless methods have rarely been developed. The conventional approaches to estimate error in meshless methods used artificial integration cells to evaluate error energy norms [Gavete, L.; Cuesta, J. L.; Ruiz, A. (2002)], but the use of such integration cells obviously weaken the advantage of the meshless methods which does not require any artificial mesh structures. In the present study, we obtained the approximated solutions of electrostatic problems us-

ing the FMLSRK method, and estimated the error distribution of grid or random node sets by a recovery-based a posteriori error estimation technique, which is based on moving least square (MLS) method and energy norm. The proposed error estimation technique does not require any artificial integration cells, but recover the exact solutions inside a virtual area defined by a dilation parameter and node density. Simulations on two typical electrostatic examples demonstrate that the proposed technique is able to estimate relative errors of approximated solutions reasonably and be applied successfully to the adaptive node refinement process.

## 2 FMLSRK method

The FMLSRK method is a kind of meshless method which can solve Poisson, stationary incompressible Stokes, and various electromagnetic problems [Kim, D. W.; Kim, Y. (2003)], [Kim, D. W.; Kim, H. K. (2004)]. Although both Galerkin formulation and point collocation scheme may be applied to implement the FMLSRK method, point collocation is better in efficiency than the Galerkin method [Kim, D. W.; Kim, H. K. (2004)]. In FMLSRK, a locally approximated solution at near can be expressed as follows:

$$U^h(\mathbf{x}, \bar{\mathbf{x}}) = \mathbf{P}_m^T \left( \frac{\mathbf{x} - \bar{\mathbf{x}}}{\rho} \right) M^{-1}(\bar{\mathbf{x}}) \sum_{I=1}^{NP} \mathbf{P}_m \left( \frac{\mathbf{x}_I - \bar{\mathbf{x}}}{\rho} \right) (1/\rho^n) \Phi(\mathbf{x}_I - \bar{\mathbf{x}}) u(\mathbf{x}_I). \quad (1)$$

where  $\mathbf{P}_m$  is a complete basis polynomial vector up to order  $m$ ,  $\rho$  is a constant called a dilation parameter, which controls the influence region of a shape function,  $NP$  is the number of points in the local area,  $u$  is the solution at  $\mathbf{x}$ ,  $n$  is the dimension of the problem, and moment matrix is given as

$$M(\bar{\mathbf{x}}) = \sum_{I=1}^{NP} \mathbf{P}_m \left( \frac{\mathbf{x}_I - \bar{\mathbf{x}}}{\rho} \right) \mathbf{P}_m^T \left( \frac{\mathbf{x}_I - \bar{\mathbf{x}}}{\rho} \right) (1/\rho^n) \Phi(\mathbf{x}_I - \bar{\mathbf{x}}), \quad (2)$$

where the window function is defined as

$$\Phi(x) = \begin{cases} (1 - \|x\|)^j, & \text{when } \|x\| < 1, j > 0 \\ 0, & \text{otherwise} \end{cases} \quad (3)$$

To implement the point collocation scheme, it is sometimes necessary to obtain higher order derivatives of shape functions because higher order basis functions can result in more accurate solutions. However, it is computationally expensive to calculate all the higher order basis functions. Compared to the other meshless methods, FMLSRK method has a powerful characteristic that it can evaluate all derivatives of the shape functions up to the order of the basis polynomials in a single equation simultaneously [Kim, D. W.; Kim, Y. (2003)], [Kim, D. W.; Kim, H. K. (2004)]. The  $\alpha$ -th derivatives of the local approximation Eq.1 with respect to  $\mathbf{x}$  is

$$D^\alpha U^h(\mathbf{x}, \bar{\mathbf{x}}) = \left[ D^\alpha \mathbf{P}_m^T \left( \frac{\mathbf{x} - \bar{\mathbf{x}}}{\rho} \right) \right] M^{-1}(\bar{\mathbf{x}}) \sum_{I=1}^{NP} \mathbf{P}_m \left( \frac{\mathbf{x}_I - \bar{\mathbf{x}}}{\rho} \right) (1/\rho^n) \Phi(\mathbf{x}_I - \bar{\mathbf{x}}) u(\mathbf{x}_I). \quad (4)$$

The  $\alpha$ -th derivatives of the global approximation can be obtained as follows, by taking the limit of Eq.4 as  $\bar{\mathbf{x}}$  converges to  $\mathbf{x}$  [Kim, D. W.; Kim, Y. (2003)]:

$$\begin{aligned} D^\alpha u^h(\mathbf{x}) &= \lim_{\bar{\mathbf{x}} \rightarrow \mathbf{x}} D^\alpha U^h(\mathbf{x}, \bar{\mathbf{x}}) \\ &= \frac{\alpha!}{\rho^{|\alpha|}} \mathbf{e}_\alpha^T M^{-1}(\mathbf{x}) \sum_{I=1}^{NP} \mathbf{P}_m \left( \frac{\mathbf{x}_I - \mathbf{x}}{\rho} \right) \Phi(\mathbf{x}_I - \mathbf{x}) u(\mathbf{x}_I), \end{aligned} \quad (5)$$

where,  $\mathbf{e}_\alpha = (0, \dots, 1, \dots, 0)^T$  is the  $\alpha$ -th unit vector. We defined the  $\alpha$ -th correction function  $C_\alpha$  and  $\alpha$ -th kernel function  $\mathcal{K}_\alpha$  as

$$C_\alpha(\rho, \mathbf{x}_I - \mathbf{x}, \mathbf{x}) = \frac{\alpha!}{\rho^{|\alpha|}} \mathbf{e}_\alpha^T M^{-1}(\mathbf{x}) \mathbf{P}_m \left( \frac{\mathbf{x}_I - \mathbf{x}}{\rho} \right), \quad (6)$$

$$\mathcal{K}_\alpha(\rho, \mathbf{x}_I - \mathbf{x}, \mathbf{x}) = C_\alpha(\rho, \mathbf{x}_I - \mathbf{x}, \mathbf{x}) \Phi(\mathbf{x}_I - \mathbf{x}). \quad (7)$$

Finally, the  $\alpha$ -th derivatives of the global approximation can be written as

$$D^\alpha u^h(\mathbf{x}) = \sum_{I=1}^{NP} \mathcal{K}_\alpha(\rho, \mathbf{x}_I - \mathbf{x}, \mathbf{x}) u(\mathbf{x}_I). \quad (8)$$

As seen from Eq.6, Eq.7 and Eq.8, the  $\alpha$ -th derivative can be readily evaluated just by multiplying a very simple function of  $\alpha$  with a function of  $\mathbf{x}$  that is independent upon  $\alpha$ . Therefore, once the function of  $\mathbf{x}$  is evaluated, the  $\alpha$ -th

derivatives of the shape functions can be evaluated without additional heavy computations. For more detailed explanations and derivation of the FMLSRK method, please refer to the previous literatures [Kim, D. W.; Kim, Y. (2003)], [Kim, D. W.; Kim, H. K. (2004)].

### 3 Error estimation

In FEM, energy norm of  $i$ -th element  $\Omega_i$  is generally defined as

$$\|\mathbf{e}\|_i = \left[ \int_{\Omega_i} [u(\mathbf{x}) - u(\mathbf{x})^h]^T \mathbf{D}^{-1} [u(\mathbf{x}) - u(\mathbf{x})^h] d\Omega_i \right]^{1/2}, \quad (9)$$

where and are the exact and the approximated solution, respectively, and  $\|\mathbf{e}\|_i$  is the error norm of  $\Omega_i$ . In many problems, however, it is hard to obtain the exact solutions. Hence, one should estimate exact solution through various kinds of recovery methods, such as least squares [Bugeda, G. (2002)], [Boroomand, B.; Zienkiewicz, O. C. (1997)], [Uberbini, F. (2004)], [Kvamsdal T.; Okstad, K. M. (1998)], [Gavete, L.; Cuesta, J. L.; Ruiz, A. (2002)]. When using (moving) least square, the recovered solution is

$$u_{rec}(\mathbf{x}) = p^T(\mathbf{x}) \cdot (\mathbf{P}_\Omega^T \mathbf{W} \mathbf{P}_\Omega)^{-1} \mathbf{P}_\Omega^T \mathbf{W}, \quad (10)$$

where is the basis function vector at , is the matrix composed of basis function vectors at all points in the local area  $\Omega$ , and is a weight matrix. The error is then redefined as

$$\|\mathbf{e}\|_i = \left[ \int_{\Omega_i} [u_{rec} - u^h]^T \mathbf{D}^{-1} [u_{rec} - u^h] d\Omega_i \right]^{1/2}. \quad (11)$$

Since no meshes are used in meshless methods, i.e.  $\Omega_i$  is not defined, artificial integration cells which are sectioned by grid or some specific rules have been usually used for evaluating the error norm of meshless methods [Gavete, L.; Cuesta, J. L.; Ruiz, A. (2002)]. As mentioned before, however, the use of artificial integration cells may lose the powerful advantage of the meshless methods which does not need to generate artificial meshes

at all. In the present study, we adopted the concept of ‘virtual area’ and proposed a simple method to evaluate the energy norm in FMLSRK. The virtual area  $S_i$  of  $i$ -th node is determined by dividing the area of a circle whose center is  $i$ -th node and radius is the dilation parameter of the FMLSRK method by the number of nodes contained in the circle. Then, the error norm for FMLSRK is defined as

$$\|\mathbf{e}\|_i = \mathbf{e}_{p,i} S_i, \quad (12)$$

where,  $\mathbf{e}_{p,i}$  is the absolute value of the difference between the recovered and approximated solutions at  $i$ -th node. To obtain the recovered solutions at each node, we also applied the same concept (MLS) as Eq.10 except that the local area  $\Omega$  was not an integration cell as in [Gavete, L.; Cuesta, J. L.; Ruiz, A. (2002)], but the circle defined above.

For the adaptive node refinement, we need to evaluate the error distribution based upon a certain error indicator. In the present study, a local error indicator  $\eta_i$  was defined as

$$\eta_i = \|\mathbf{e}\|_i / \|\mathbf{e}\|_r, \quad (13)$$

where,  $\|\mathbf{e}\|_r$  is the desirable error norm. Since the optimal distribution of nodes means that the error norm is constant on the whole domain, or the density of error is equally distributed, the following condition should be satisfied for all  $j$  ( $j = 1, \dots, N$ ) where  $N$  is the number of nodes [Bugeda, G. (2002)]:

$$\|\mathbf{e}\|_j / \Omega_j^{1/2} = \|\mathbf{e}\| / \Omega^{1/2}, \quad (14)$$

where  $\|\mathbf{e}\|$  and  $\Omega$  are the error and area of the whole analysis domain, respectively. Since  $\|\mathbf{e}\|_j$  that satisfies Eq.14 is the desirable error  $\|\mathbf{e}\|_r$  at each node,  $\eta_i$  can be rewritten as

$$\eta_i = (\|\mathbf{e}\|_i / \|\mathbf{e}\|) (\Omega / \Omega_i)^{1/2}. \quad (15)$$

In the present study, we determined new node locations for the next adaptive analysis step according to the error indicator in Eq.15.

## 4 Results

The FMLSRK method was applied to two typical and simple electrostatic problems which are presented in Figs. 1 and 2. Those models have been frequently used to verify various error estimation techniques because of their clear singularity [Gavete, L.; Cuesta, J. L.; Ruiz, A. (2002)], [Janicke, L.; Kost A. (1996)]. The FMLSRK solutions in Figs. 1 and 2 show reasonable potential distributions as expected.

### 4.1 Application to grid node set

The proposed error estimation technique was applied to the first electrostatic problem shown in Fig. 1 and tested if the proposed error estimator works reasonably. We first applied it to a regular grid-node set consisting of 96 nodes, shown in Fig. 3(a). After obtaining the approximated solutions from the FMLSRK method, error distribution was estimated using Eq.15. The result of the error estimation for the initial node set is presented in Fig. 3(b), where the values are presented in logarithmic scale and the darker color represents the higher error regions. We can clearly see that the regions near the singularity (inner corner of the L-shape domain) are darker than the other regions, which demonstrates that the proposed error estimation technique can estimate the error distribution reasonably well.

In order to investigate the influence of the node refinement upon the estimated error distribution, we added 75 nodes to the initial node set and constructed a new node set shown in Fig. 3(c). It can be seen from the resultant error estimate shown in Fig. 3(d) that the error around the refined regions was significantly reduced. Figs. 3(e) and 3(f) show the third level node refinement (44 nodes were added) around the singular point and the resultant error distribution, respectively. It can be seen from the figures that the error can be reduced by the additional nodes as anyone can expect, which clearly demonstrates that the proposed error estimator can be used as a reasonable error estimator for adaptive meshless analysis.

If we refine the node set without estimating the errors to get the same accuracy around the cor-

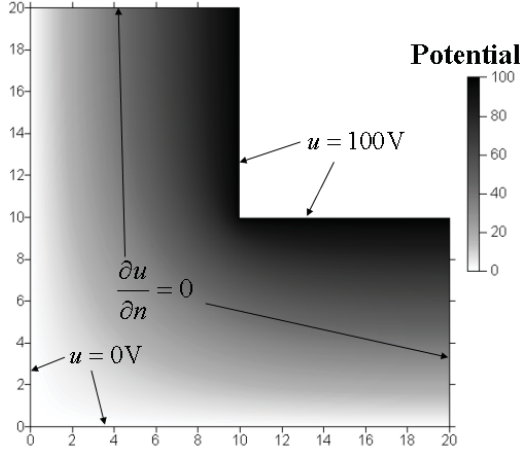


Figure 1: First electrostatic model for the FMLS-RK analysis and its solution. Both Dirichlet and Neumann boundary conditions are presented herein. This model has the singularity at the corner (10, 10)

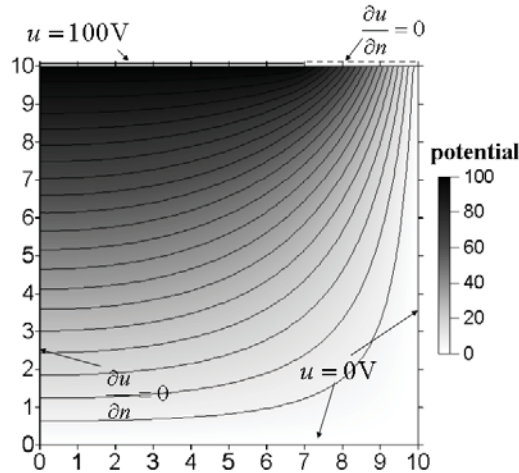


Figure 2: Second electrostatic model for the FMLS-RK analysis and its solution. Both Dirichlet and Neumann boundary conditions are presented herein. The model has the singularity at (7,10)

ner, i.e. the gap between neighboring nodes is the same as the shortest distance between two nodes in Fig. 3(e), the number of nodes would be about 2500, which explains why we need to apply the adaptive node refinement in the meshless analysis.

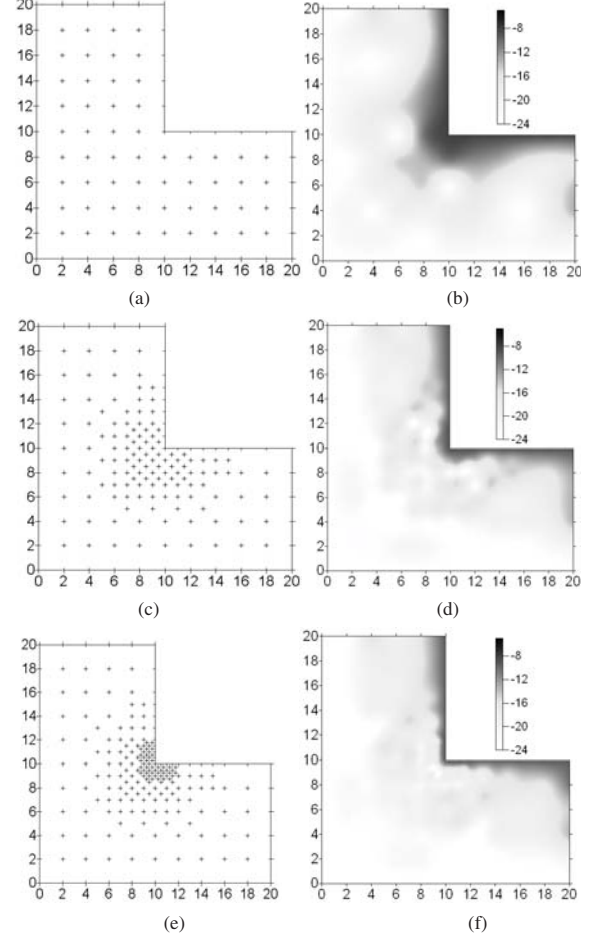


Figure 3: Error estimation and adaptive node refinement for grid node set: (a) Initial node set consisting of 96 nodes; (b) Error distribution of (a). The darker color represents the higher error; (c) First-level node refinement. Number of nodes = 171; (d) Error distribution of (c); (e) Second-level node refinement. Number of nodes = 215; (f) Error distribution of (e). The dark region was reduced by the additional nodes. In all the figures presented in this paper, logarithmic value of Eq.16 was used as the error indicator.

#### 4.2 Application to random node set

In the previous section, we applied the proposed error estimation technique to a grid node set and investigated the influence of the node refinement. In this section, we applied the proposed technique to more practical random node sets and refined node distribution based upon the estimated er-

ror distribution. Fig. 4 shows the results of the error estimation and the node set refined using the error distribution. New nodes were randomly placed around a node which has high error indicator value over a threshold. The initial node set (Fig. 4(a)) and the refined node set (Fig. 4(c)) included 141 and 231 nodes, respectively. It can be clearly observed from the Figs. 4(b) and 4(d) that regions with higher error were significantly reduced by applying the adaptive node refinement.

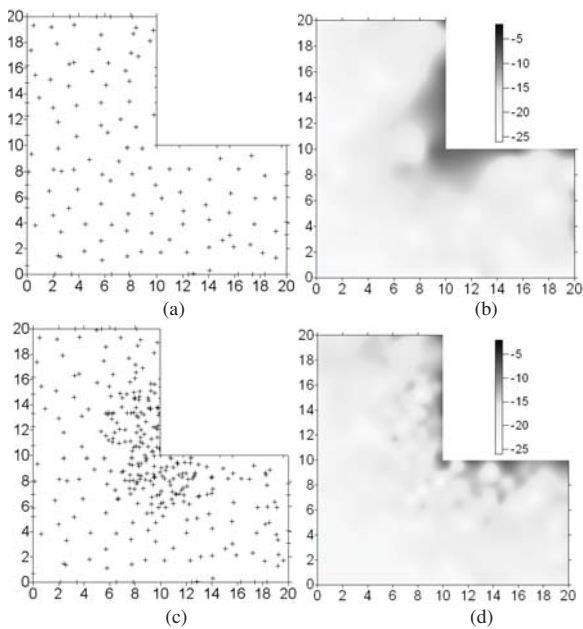


Figure 4: Error estimation and adaptive node refinement for a random node set. New nodes were placed beside a node which has high error indicator: (a) Initial node set consisting of 141 nodes; (b) Error distribution of (a). The darker color represents the higher error; (c) Refined node distribution consisting of 231 nodes; (d) Error distribution of (c).

We then applied the proposed error estimation technique to another electrostatic problem presented in Fig. 2. This model has the singularity at the point between Dirichlet and Neumann condition on the upper boundary. The node distributions and the resultant error distributions are presented in Fig. 5 in the same way as the previous example. The use of adaptive node refinement did

not only reduce the higher error regions, but also made the error distribution more homogeneous.

Please note from Eq.14 that the goal of the adaptive node refinement was flattening the error distribution by decreasing high-error region. In the L-shape electrostatic model with random node set (Fig. 4), the standard deviations of errors were reduced from 5.02 to 4.21. In the other example (Fig. 5), the standard deviations were also reduced from 6.21 to 4.65.

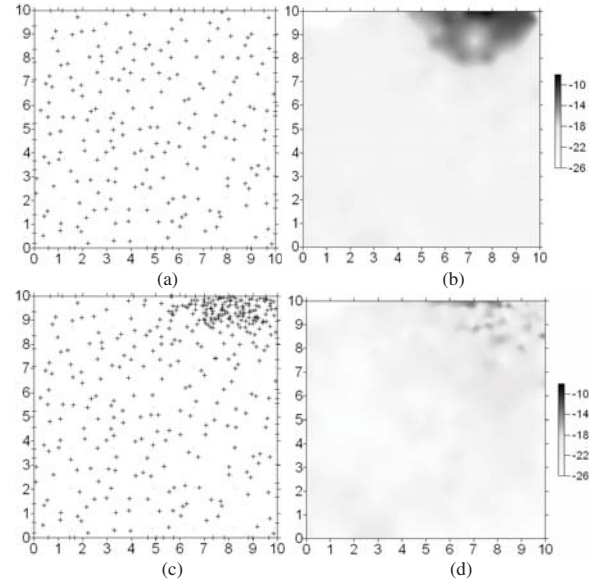


Figure 5: Error estimation and adaptive node refinement for random node set (second electrostatic example): (a) Initial node set consisting of 249 nodes; (b) Error distribution of (a); (c) Refined node distribution consisting of 400 nodes; (d) Error distribution of (c).

## 5 Conclusion

In this paper, a recovery-based *a posteriori* error estimation technique for FMLSRK method is proposed. The proposed error estimator evaluated by MLS in virtual areas was applied to two electrostatic examples with singularity. It was verified from the simulation studies that the suggested error estimation can not only estimate error distribution reasonably, but also be successfully used for the adaptive node refinement. Although the pro-

posed error estimator was applied only to FMLS-RK method, it can be generally applied to other meshless methods if the dilation parameters are determined *a priori*.

## References

- Atluri S.N., Kim H.G., Cho J.Y.** (1999): A critical assessment of the truly meshless local Petrov-Galerkin(MLPG) and local boundary integral equation(LBIE) methods. *Comput Mech*, vol. 24, pp. 348-372.
- Atluri S.N., Shen S.** (2002): The meshless local Petrov-Galerkin(MLPG) method: A simple & Less-costly alternative to the finite element and boundary element methods. *CMES: Computer Modeling in Engineering & Science*, vol. 3(1): pp. 11-51.
- Boroomand, B.; Zienkiewicz, O. C.** (1997): Recovery by equilibrium in patches (REP) *Int J Numer Meth Engng*, vol. 40, pp. 137-164.
- Bugeda, G.** (2002): A comparison between new adaptive remeshing strategies based on point wise stress error estimation and energy norm error estimation. *Commun Numer Meth Engng*, vol. 18, pp. 469-482.
- Duarte, C. A.; Oden, J. T.** (1996): An h-p adaptive method using clouds. *Comput Meth Appl Mech Eng*, vol. 139, pp. 237-262.
- Gingold, R. A.; Monaghan, J. J.** (1997): Smoothed particle hydrodynamics: theory and application to non-spherical stars. *Mon Not R astr Soc*, vol. 181, pp. 375-389.
- Gavete, L.; Cuesta, J. L.; Ruiz, A.** (2002): A procedure for approximation of the error in the EFG method. *Int J Numer Meth Engng*, Vol. 53, pp. 677-690.
- Janicke, L.; Kost A.** (1996): Error estimation and adaptive mesh generation in the 2D and 3D finite element method. *IEEE Trans Magn*, vol. 32, No. 3, pp. 1334-1337.
- Kim, D. W.; Kim, Y.** (2003): Point collocation methods using the fast moving least-square reproducing kernel approximation. *Int J Numer Meth Engng*, vol. 56, pp.1445-1464.
- Kim, D. W.; Kim, H. K.** (2004): Point collocation method based on the FMLS-RK approximation for electromagnetic field analysis. *IEEE Trans Magn*, vol. 40, no. 2, pp. 1029-1032.
- Kvamsdal T.; Okstad, K. M.** (1998): Error estimation based on superconvergent patch recovery using statically admissible stress fields. *Int J Numer Meth Engng*, vol. 42, pp. 443-472.
- Lu, Y. Y.; Belytschko, T.; Gu, L.** (1994): A new implementation of the element free Galerkin method. *Comput Meth Appl Mech Eng*, vol. 113, pp. 397-414.
- Liu, W. K.; Jun, S.; Zhang, Y. F.** (1995): Reproducing kernel particle methods. *Int J Numer Meth Fl*, vol. 20. pp. 1081-1106.
- Liu, W. K.; Li, S; Belytschko, T.** (1996): Moving least square reproducing kernel methods (I) methodology and convergence. *Comput Meth Appl Mech Eng*, vol. 143. pp. 422-433.
- Lin H., Atluri S.N.** (2000): Meshless local Petrov-Galerkin(MLPG) method for convection-diffusion problems. *CMES: Computer Modeling in Engineering & Science*, vol. 1(2): pp. 45-60.
- Lin H., Atluri S.N.** (2001): The meshless local Petrov-Galerkin(MLPG) method for solving incompressible Navier-Stokes equations. *CMES: Computer Modeling in Engineering & Science*, vol. 2(2): pp. 117-142.
- Melenk, J. M.; Babuška, I.** (1996): The partition of unity finite element method: basic theory and applications. *Int J Numer Meth Engng*, vol. 139. pp. 289-314.
- Shu C., Ding H., Yeo K.S.** (2005): Computation of incompressible Navier-Stokes equations by local RBF-based differential quadrature method. *CMES: Computer Modeling in Engineering & Science*, vol. 7(2): pp. 195-205.
- Uberbini, F.** (2004): Patch recovery based on complementary energy. *Int J Numer Meth Engng*, vol. 59, pp. 1501-1538.

